

## UNTWISTING THE TORNADO: X-RAY IMAGING AND SPECTROSCOPY OF G357.7–0.1

B. M. GAENSLER,<sup>1</sup> J. K. J. FOGEL,<sup>2</sup> P. O. SLANE,<sup>1</sup> J. M. MILLER,<sup>1</sup>  
R. WIJNANDS,<sup>3</sup> S. S. EIKENBERRY,<sup>4</sup> AND W. H. G. LEWIN<sup>5</sup>

*Accepted to ApJ Letters on 2003 Jul 08*

### ABSTRACT

We report on the detection of X-ray emission from the unusual Galactic radio source G357.7–0.1 (the “Tornado”). Observations made with the *Chandra X-ray Observatory* demonstrate the presence of up to three sources of X-ray emission from the Tornado: a relatively bright region of dimensions  $2' \times 1'$  coincident with and interior to the brightest radio emission at the “head” of the Tornado, plus two fainter extended regions possibly associated with the Tornado’s “tail”. No X-ray point sources associated with the Tornado are seen down to a  $3\sigma$  luminosity (0.5–10 keV) of  $1 \times 10^{33}$  erg s<sup>-1</sup>, for a distance to the system of 12 kpc. The spectrum of the brightest region of X-rays is consistent with a heavily absorbed ( $N_H \approx 10^{23}$  cm<sup>-2</sup>) thermal plasma of temperature  $kT \sim 0.6$  keV; an absorbed power law can also fit the data, but implies an extremely steep photon index. From these data we tentatively conclude that the Tornado is a supernova remnant (SNR), although we are unable to rule out the possibility that the Tornado is powered either by outflows from an X-ray binary or by the relativistic wind of an unseen pulsar. Within the SNR interpretation, the head of the Tornado is a limb-brightened radio shell containing centrally-filled thermal X-rays and which is interacting with a molecular cloud. We therefore propose that the Tornado is a “mixed morphology” supernova remnant. The unusual tail component of the Tornado remains unexplained in this interpretation, but might result from expansion of the SNR into an elongated progenitor wind bubble.

*Subject headings:* ISM: individual (G357.7–0.1) — ISM: supernova remnants

### 1. INTRODUCTION

The bright radio source G357.7–0.1 is extended, has high levels of polarization and shows a non-thermal spectrum, properties which at first led to its classification as a supernova remnant (SNR). However, high-resolution images revealed a bizarre axial “head-tail” structure (Shaver et al. 1985; Helfand & Becker 1985; top panel of Fig 1), for which this source was nicknamed “the Tornado”. The morphology of the Tornado is very different from the approximately circular morphologies seen in other SNRs. This has led to various claims that the Tornado is an exotic SNR expanding into an unusual environment, is a nebula powered by a high velocity pulsar, or results from precessing jets from an X-ray binary (e.g. Manchester 1987; Shull, Fesen, & Saken 1989; Stewart et al. 1994).

Recent observations have provided some new clues. Frail et al. (1996) detected a 1720-MHz OH maser from the “head” of the Tornado. The 1720 MHz emission, when seen without the other OH maser lines, is produced by shocks propagating into molecular clouds; further evidence for an interaction with molecular material is provided by the presence of emission from <sup>13</sup>CO 1–0 and shock-excited 2.12- $\mu$ m H<sub>2</sub> at this same position and velocity (Lazendic et al. 2003). The maser velocity, also now confirmed by H I absorption measurements (Brogan & Goss 2003), implies a distance to the Tornado of 12 kpc.

Despite these new data, the Tornado still defies classification. Most problematic has been the failure to detect emission in other wavebands. We consequently examined archival ASCA data of this region, and identified a weak ( $\sim 3\sigma$ ) X-ray source coincident with the Tornado’s head; this marginal detec-

tion was also briefly noted by Yusef-Zadeh et al. (2003). We here present an observation of the Tornado with the *Chandra X-ray Observatory*, aimed at confirming this source of X-rays, and studying its morphology and spectrum.

### 2. OBSERVATIONS AND RESULTS

The Tornado was observed with *Chandra* on 2002 May 07. We used the ACIS-I detector, consisting of an array of four front-illuminated CCDs and giving a field of view approximately  $17' \times 17'$ . The aimpoint, located near the center of the array, corresponded to coordinates RA (J2000) 17<sup>h</sup>40<sup>m</sup>15<sup>s</sup>.33, Decl. (J2000)  $-30^\circ 57' 59''$ .2. The effective exposure time was 20 723 seconds, and was free of background flares.

#### 2.1. Imaging

Data were analyzed using CIAO v2.3. We used the level-1 events supplied by the Chandra X-ray Center (CXC), and then corrected them for charge-transfer inefficiency using standard CXC routines. An image was then formed using events in the energy range 0.3 to 10 keV; point sources in this image were identified using the *wavdetect* algorithm within CIAO. To highlight diffuse emission, we applied the adaptive smoothing algorithm *csmooth*. We corrected for off-axis vignetting and for the variable exposure produced by chip gaps and bad pixels by forming an exposure map, which we then smoothed with the same kernel as was applied to the image. Applying the smoothed exposure map to the smoothed image resulted in a flux-calibrated image of diffuse emission. The resulting X-ray image is shown in the lower panel of Figure 1, demonstrating

<sup>1</sup>Harvard-Smithsonian Center for Astrophysics, 60 Garden Street MS-6, Cambridge, MA 02138; bgaensler@cfa.harvard.edu

<sup>2</sup>Harvard College, Cambridge MA 02138

<sup>3</sup>School of Physics and Astronomy, University of St Andrews, St Andrews, Fife KY16 9SS, United Kingdom

<sup>4</sup>Department of Astronomy, University of Florida, 211 Bryant Space Science Center, Gainesville FL 32611

<sup>5</sup>Physics Department and Center for Space Research, Massachusetts Institute of Technology, 70 Vassar Street, Cambridge MA 02139

that faint emission is detected from three distinct regions coincident with the Tornado, which we label A, B and C.

The brightest X-rays are from region A, lying near the “head” of the Tornado, and comprising a  $\sim 2' \times 1'$  elliptical region elongated along a position angle  $\sim 150^\circ$  (north through east). Comparison with radio data shows that these X-rays are wholly contained within the head region, occupying the western half of the head’s interior. While region A is brighter and more concentrated at its south-eastern tip, no unresolved source is identified in this region by `wavdetect`, nor is apparent by visual inspection of the unsmoothed image.

Regions B and C represent two other possible sources of extended X-rays from the Tornado, located  $\sim 2'$  east of the head region. Region B is a very faint circular clump of extent  $\sim 30''$ , while region C is a brighter and more elongated feature of extent  $\sim 1'$ . Given the faintness of regions B and C, we simply note their existence, and defer detailed studies of these regions until deeper observations have been performed. The `wavdetect` algorithm identifies two X-ray point sources lying within the radio boundaries of the Tornado, as marked in Fig 1. Both sources are of marginal significance, each containing only 5–6 counts.

### 2.2. Spectroscopy

Of the three extended regions of X-ray emission identified in §2.1, only region A is bright enough from which to obtain a useful spectrum. Events were extracted from an elliptical extraction region of dimensions  $150'' \times 120''$  centered on this emission, and the data (source plus background) were then re-grouped so that there were at least 50 counts in each energy bin. The effective area for this source spectrum was determined by weighting by the brightness of the source over the extraction region using the CIAO task `mkwarf`. The local background was determined by extracting a spectrum from an adjacent emission-free region of the CCD immediately to the southwest of region A.

The corresponding spectrum contains  $162 \pm 37$  background-subtracted counts, which fall into 12 bins spread over the energy range 0.3–10 keV. We fit two simple models to this spectrum: a power law, and a Raymond-Smith plasma in collisionally ionized equilibrium,<sup>6</sup> both modified by foreground photoelectric absorption. Both models give good fits to the data, the parameters for which are listed in Table 1. However, the implied photon index for the best power law fit is unusually steep,  $\Gamma > 4.5$  at 90% confidence. In Table 1 we also present power law fits for fixed photon indices  $\Gamma = 2.3$  and  $\Gamma = 3.5$  (representing extreme value for observed sources; see §§3.2 & 3.3), which give comparatively poor fits to the data.

## 3. DISCUSSION

We have clearly identified X-ray emission from the head of the Tornado; the observed count-rate is consistent (to within  $\sim 50\%$ ) with the level of emission suggested from archival ASCA data. Although we detect relatively few X-ray photons from the Tornado, these data provide new constraints on the nature of this complicated source.

### 3.1. Outflows from an X-ray binary?

Stewart et al. (1994) propose that the Tornado is powered by twin outflows from a central X-ray binary, presumably located in the center of and along the symmetry axis of the overall radio

nebula, and which generate opposed precessing jets as is seen for SS 433 in the SNR W50 (e.g. Margon 1984). We argue in §3.3 below that region A has a thermal spectrum. In the context of the situation proposed by Stewart et al. (1994), these thermal X-rays might represent the working surface where a collimated outflow from the central source collides and interacts with surrounding gas, as is seen at the termination of the eastern lobe of W50 (Brinkmann, Aschenbach, & Kawai 1996; Safi-Harb & Ögelman 1997).

Of immediate concern for such a model is that no bright unresolved X-ray emission, corresponding to a central powering source, is seen along the axis of the Tornado. The  $3\sigma$  upper limit on the count-rate from any such source is  $\approx 5 \times 10^{-4}$  cts  $s^{-1}$  in the energy range 0.3–10 keV. Assuming a foreground absorbing column density of  $N_H \approx 1 \times 10^{23}$   $cm^{-2}$  (see §3.3 below) and a power-law spectrum with photon index  $\Gamma = 2$ , we infer an unabsorbed flux (0.5–10 keV) for such a source  $f_X \lesssim 6 \times 10^{-14}$  ergs  $cm^{-2}$   $s^{-1}$ , which implies an upper limit on the X-ray luminosity (0.5–10 keV)  $L_X \lesssim 1 \times 10^{33}$  ergs  $s^{-1}$  at a distance of 12 kpc.

From this non-detection an exact analogy with SS 433 can immediately be ruled out: even when not in outburst, such a source would have an X-ray luminosity  $L_X \sim 10^{36}$  ergs  $s^{-1}$  and a 1.4-GHz flux density  $\sim 100$  mJy (see Margon 1984 and references therein), which would have been easily detected in *Chandra* and VLA observations of the Tornado, respectively. However, we below note two other X-ray binaries known to generate outflows, which if embedded in the Tornado might not be directly detectable.

The recently discovered high-mass X-ray binary LS 5039 generates steady jets of velocity  $\sim 0.2c$  and kinetic luminosity  $\sim 10^{37}$  ergs  $s^{-1}$  (Paredes et al. 2000), which is consistent with the rate of energy input required to power the radio emission seen from the Tornado (Helfand & Becker 1985). The X-ray luminosity of LS 5039 possibly varies as a function of orbital phase, but at its minimum is only slightly higher than the upper limit determined for any point source in the Tornado (Reig et al. 2003). At a distance of 12 kpc, the 1.4-GHz flux density of this source would only be 1–3 mJy (Martí, Paredes, & Ribó 1998), too faint to be seen in existing VLA radio images of this region.

The low-mass X-ray binary 4U 1755-338 is currently in a quiescent state with  $L_X < 4 \times 10^{31}$  ergs  $s^{-1}$ , but previously underwent an active phase lasting several decades, in which it generated X-ray jets  $\sim 4$  pc in extent (Angelini & White 2003). The Tornado could similarly have been powered by a period of prolonged activity, but is now quiescent. Jets of the surface brightness seen for 4U 1755-338 would be too faint to be detected here.

We note that an alternative X-ray binary model has been proposed by Helfand & Becker (1985), who argue that the Tornado is powered by source at the very western edge of the head, and that the high velocity of the binary then gives the Tornado its unusual appearance. The arguments invoked above can explain the failure to detect X-ray emission from the binary itself. However, in this model the energetic interaction between the outflow and its surroundings should occur only at the very western edge of the Tornado. In such a situation, there is no simple explanation for the presence of extended X-ray emission from region A, since this should be neither a region of active particle acceleration nor an area in which shock-heated gas is produced. We therefore think this possibility unlikely.

<sup>6</sup>More complicated thermal models including non-equilibrium ionization give near identical best-fit parameters.

### 3.2. A pulsar powered nebula?

Shull et al. (1989) have argued that the Tornado is a pulsar wind nebula (PWN) powered by a high-velocity pulsar. In such a situation, the pulsar is presumed to be inside of or to the west of the head of the Tornado. We can consequently expect to see extended synchrotron X-ray emission from a surrounding PWN, plus possibly unresolved magnetospheric X-ray emission from the pulsar itself.

Region A clearly corresponds to X-ray emission in the expected location for this interpretation, and its spectrum can be well-fitted by a power law characteristic of synchrotron emission. However, all known PWNe show power law X-ray spectra with photon indices in the range  $1.3 \lesssim \Gamma \lesssim 2.3$  (Gotthelf 2003); Table 1 shows that a photon index even at the upper limit of this range,  $\Gamma = 2.3$ , gives a comparatively poor fit, which we can exclude at the  $\sim 2.3\sigma$  level. While more data are needed to confirm whether this source indeed has an anomalously steep spectrum, this measurement suggests that the properties of region A are not consistent with those expected for a pulsar-powered nebula. We note that while we detect no point source embedded in region A, the corresponding upper limit  $L_X \lesssim 1 \times 10^{33}$  ergs  $s^{-1}$  (see §3.1 above) is above the X-ray luminosities of many young pulsars (Possenti et al. 2002).

### 3.3. A supernova remnant

The Tornado shows bright, polarized, limb-brightened radio emission with a non-thermal spectrum, properties which resulted in its original classification as a SNR. However, one must then explain its bizarre and unique morphology.

In a dense ambient medium a supernova progenitor's space velocity can take it near the edge of, or even outside of, its circumstellar bubble before the star explodes. The SNR resulting from such a system will have a highly elongated axial morphology (Różyczka et al. 1993; Brighenti & D'Ercole 1994), resembling that seen for the Tornado. The OH maser identified towards this source by Frail et al. (1996), along with the recent detection of shock-excited 2.12- $\mu$ m  $H_2$  emission and surrounding  $^{13}CO$  emission by Lazendic et al. (2003), all argue that indeed the Tornado is expanding into a dense environment.

For a SNR interpretation there are several different possibilities for the X-ray emission expected. We might see limb-brightened synchrotron emission from shock-accelerated electrons (e.g. G347.3–0.5; Slane et al. 1999), limb-brightened thermal emission from shock-heated ambient gas (e.g. 1E 0102.2–7219; Hughes, Rakowski, & Decourchelle 2000), or centrally-filled thermal emission from hot gas in the interior, corresponding to a so-called “mixed morphology” or “thermal composite” SNR (e.g. W44; Rho et al. 1994).

The X-ray photon index for synchrotron-emitting SNRs is in the range  $2.5 \lesssim \Gamma \lesssim 3.5$  (see Petre 2001 for a review) which, as for the case of a PWN in §3.2, is distinctly flatter than the best-fit power law observed. On the other hand, the temperature of  $kT \sim 0.6$  keV implied by thermal models is quite reasonable for thermally emitting SNRs, as is the corresponding unabsorbed X-ray luminosity (0.5–10 keV) of  $L_X \sim 10^{36}$  erg  $s^{-1}$  for a distance of 12 kpc. The foreground column  $N_H \approx 10^{23}$   $cm^{-2}$  is high, but is well below the total integrated column in this direction of  $N_H \approx 1.5 \times 10^{23}$   $cm^{-2}$  (Dickey & Lockman 1990).

If we identify the head of the Tornado as a limb-brightened radio SNR, then the emission seen with *Chandra* originates wholly from the SNR interior, and we correspondingly can tentatively classify the Tornado as a mixed morphology SNR

(as had been earlier speculated by Yusef-Zadeh et al. 2003 from the possible presence of *ASCA* emission). Whether such centrally-filled thermal X-rays are produced by evaporation of dense clouds overrun by the shock, through thermal conduction in the interior, or via some other process is currently controversial (Rho & Petre 1998). However, regardless of the mechanism invoked, there have been repeated arguments that such a SNR is the result of an interaction with a dense molecular cloud (Green et al. 1997; Rho & Petre 1998; Yusef-Zadeh et al. 2003). The OH maser, 2.12- $\mu$ m  $H_2$  and  $^{13}CO$  emission seen here all support this interpretation.

Wardle (1999) has pointed out that the soft X-ray emission produced by a mixed morphology SNR can produce the ionizing flux  $\zeta \gtrsim 10^{-16}$   $s^{-1}$  needed to disassociate  $H_2O$  and produce the OH seen in maser emission. At a distance of 12 kpc, the maser produced by the Tornado is  $\sim 3.5$  pc from the source of X-rays, implying a flux as seen by the OH maser  $f_X \sim 6 \times 10^{-4}$  ergs  $cm^{-2}$   $s^{-1}$ . The consequent ionizing flux is  $\zeta = N_e \sigma f_X \sim 3 \times 10^{-15}$   $s^{-1}$ , where  $N_e \approx 30$  keV $^{-1}$  is the number of electrons produced per keV of ionization and  $\sigma \approx 2.6 \times 10^{-22}$  is the photoabsorption cross-section of hydrogen at 1 keV (Wardle 1999). This rate of ionization is more than sufficient to convert water into OH molecules.

## 4. CONCLUSIONS

A short observation of G357.7–0.1 with the *Chandra X-ray Observatory* has confirmed the presence of X-ray emission from this remarkable object. The brightest region of X-rays from this source is clearly extended, seems to sit within the shell of emission defined by the “head” of the radio source, and has a highly absorbed spectrum consistent with being either an extremely steep power law or a collisionally ionized plasma at a temperature  $\sim 0.6$  keV.

We have considered the possibility of the Tornado being powered by jets from an X-ray binary, of corresponding to the synchrotron nebula powered by an energetic rotation-powered pulsar, or of representing an unusually-shaped supernova remnant. While the available data do not allow us to definitively rule out any of these alternatives, the spectrum and morphology of the X-ray emission seen by *Chandra*, when combined with evidence at other wavebands for the interaction of a shock with a molecular cloud, all suggest that the head of the Tornado is a “mixed morphology” supernova remnant, producing thermal X-rays from the interior of a limb-brightened radio shell, and expanding into a dense and possibly complicated distribution of ambient gas.

This argument provides a reasonably simple interpretation for the “head” of the Tornado, but the bizarre morphology of the “tail” remains unexplained. We speculate that the Tornado might result from expansion of a SNR into a highly elongated progenitor wind bubble, but explanations involving pre-existing helical magnetic fields, or high-speed outflows from a still unseen central source, can also not be discounted. Deep X-ray observations with *Chandra* and *XMM* are needed to better determine the morphology and spectrum of X-rays from the head, and to study the possible X-ray emission from the tail.

We thank Dan Harris, Jasmina Lazendic and Fred Seward for useful discussions, and Crystal Brogan for supplying us with her radio images of the Tornado. This work was supported by NASA through SAO grant GO2-3041X (BMG) and by the NSF (JMM).

## REFERENCES

- Angelini, L. & White, N. E. 2003, *ApJ*, 586, L71.  
 Bałucińska-Church, M. & McCammon, D. 1992, *ApJ*, 400, 699.  
 Brighenti, F. & D’Ercole, A. 1994, *MNRAS*, 270, 65.  
 Brinkmann, W., Aschenbach, B., & Kawai, N. 1996, *A&A*, 312, 306.  
 Brogan, C. L. & Goss, W. M. 2003, *AJ*, 125, 272.  
 Dickey, J. M. & Lockman, F. J. 1990, *Ann. Rev. Astr. Ap.*, 28, 215.  
 Frail, D. A., Goss, W. M., Reynoso, E. M., Giacani, E. B., Green, A. J., & Otrupcek, R. 1996, *AJ*, 111, 1651.  
 Gotthelf, E. V. 2003, *ApJ*, 591, 361.  
 Green, A. J., Frail, D. A., Goss, W. M., & Otrupcek, R. 1997, *AJ*, 114, 2058.  
 Helfand, D. J. & Becker, R. H. 1985, *Nature*, 313, 118.  
 Hughes, J. P., Rakowski, C. E., & Decourchelle, A. 2000, *ApJ*, 543, L61.  
 Lazendic, J., Burton, M., Yusef-Zadeh, F., Wardle, M., Green, A., & Whiteoak, J. 2003, *Astron. Nachr.*, 324, in press (astro-ph/0304329).  
 Manchester, R. N. 1987, *A&A*, 171, 205.  
 Margon, B. 1984, *Ann. Rev. Astr. Ap.*, 22, 507.  
 Martí, J., Paredes, J. M., & Ribó, M. 1998, *A&A*, 338, L71.  
 Paredes, J. M., Martí, J., Ribó, M., & Massi, M. 2000, *Science*, 288, 2340.  
 Petre, R. 2001, in *Young Supernova Remnants* (AIP Conference Proceedings Volume 565), ed. S. S. Holt & U. Hwang, (New York: AIP), p. 360.  
 Possenti, A., Cerutti, R., Colpi, M., & Mereghetti, S. 2002, *A&A*, 387, 993.  
 Raymond, J. C. & Smith, B. W. 1977, *ApJS*, 35, 419.  
 Reig, P., Ribó, M., Paredes, J. M., & Martí, J. 2003, *A&A*, 405, 285.  
 Rho, J. & Petre, R. 1998, *ApJ*, 503, L167.  
 Rho, J., Petre, R., Schlegel, E., & Hester, J. 1994, *ApJ*, 430, 757.  
 Różyczka, M., Tenorio-Tagle, G., Franco, J., & Bodenheimer, P. 1993, *MNRAS*, 261, 674.  
 Safi-Harb, S. & Ögelman, H. 1997, *ApJ*, 483, 868.  
 Shaver, P. A., Salter, C. J., Patnaik, A. R., van Gorkom, J. H., & Hunt, G. C. 1985, *Nature*, 313, 113.  
 Shull, J. M., Fesen, R. A., & Saken, J. M. 1989, *ApJ*, 346, 860.  
 Slane, P., Gaensler, B. M., Dame, T. M., Hughes, J. P., Plucinsky, P. P., & Green, A. 1999, *ApJ*, 525, 357.  
 Stewart, R. T., Haynes, R. F., Gray, A. D., & Reich, W. 1994, *ApJ*, 432, L39.  
 Wardle, M. 1999, *ApJ*, 525, L101.  
 Yusef-Zadeh, F., Wardle, M., Rho, J., & Sakano, M. 2003, *ApJ*, 585, 319.

TABLE 1

SPECTRAL FITS TO X-RAY EMISSION FROM THE HEAD OF THE TORNADO.

Model	$N_H$ ( $10^{22}$ cm $^{-2}$ )	$\Gamma / kT$ (keV)	$f_x$ ( $10^{-11}$ erg cm $^{-2}$ s $^{-1}$ )	$\chi^2_\nu / \nu$
RS	$10^{+7}_{-4}$	$0.6^{+0.8}_{-0.3}$	$\sim 5.1$	$10.2/9 = 1.1$
PL	$12^{+6}_{-5}$	$> 4.5$	$> 1.2$	$10.8/9 = 1.2$
PL	$\sim 3.4$	2.3 (fixed) <sup>a</sup>	$\sim 0.05$	$20.3/10 = 2.0$
PL	$5 \pm 1$	3.5 (fixed) <sup>a</sup>	$\sim 0.2$	$15.7/10 = 1.6$

<sup>a</sup>See §§3.2 and 3.3 for details.

Uncertainties and lower limits are all at 90% confidence. All models assume interstellar absorption using the cross-sections of Bałucińska-Church & McCammon (1992), assuming solar abundances. Models used: “PL” indicates a power law of the form  $f_\epsilon \propto \epsilon^{-\Gamma}$  where  $\Gamma$  is the photon index; “RS” indicates a Raymond-Smith spectrum of temperature  $T$  (Raymond & Smith 1977). Fluxes are for the energy range 0.5–10 keV, and have been corrected for interstellar absorption.

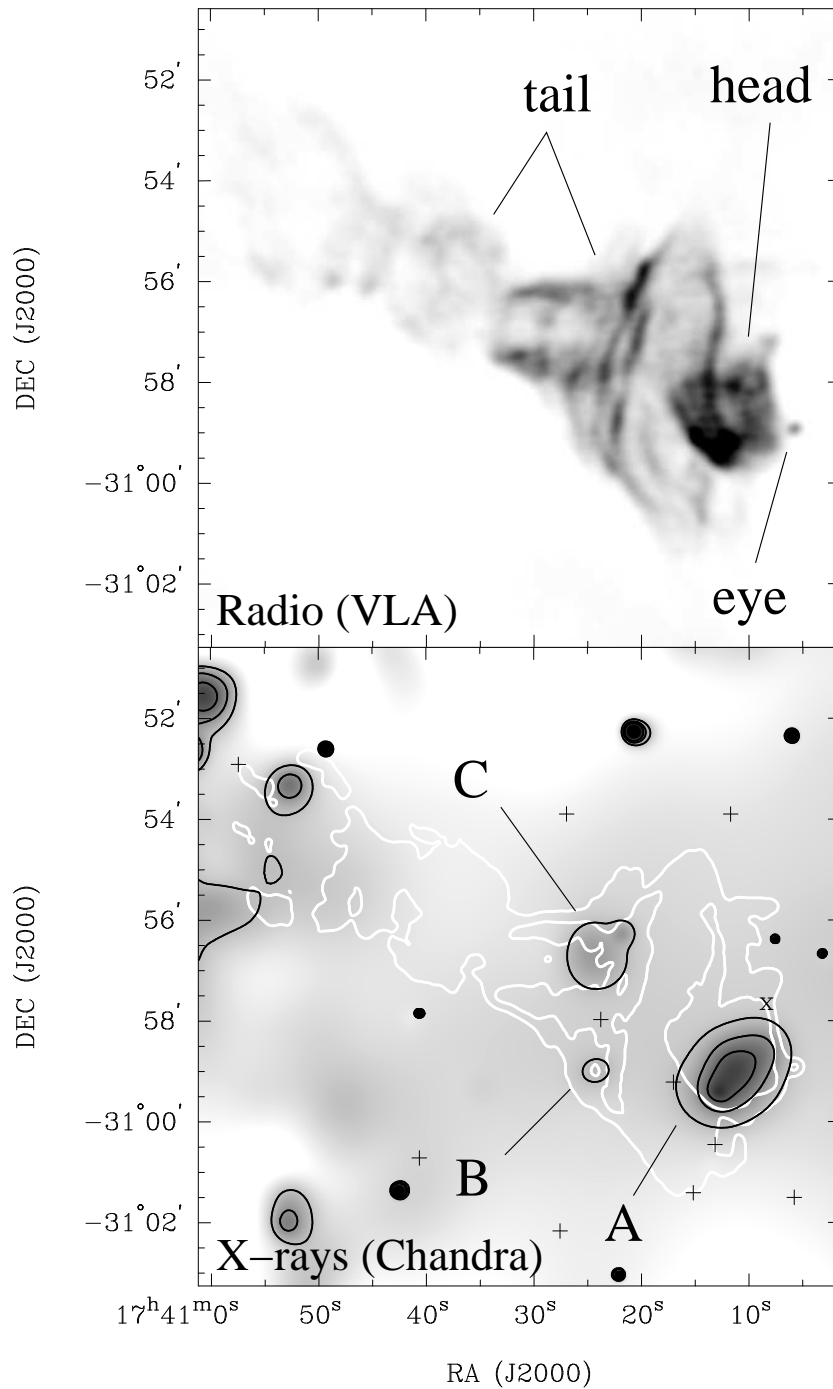


FIG. 1.— Radio and X-ray images of G357.7-0.1 (“the Tornado”). The top panel shows a 1.4-GHz VLA image of the Tornado, corrected for primary beam attenuation and with a spatial resolution of  $14'' \times 11''$  (Brogan & Goss 2003). (The “eye” of the Tornado, is an unrelated H II region; Brogan & Goss 2003.) The image in the bottom panel shows *Chandra* ACIS-I data in the energy range 0.3–10 keV after exposure correction and adaptive smoothing. In the bottom panel, black contours represent X-ray emission at levels of 76%, 84% and 92% of the peak brightness of region A, while white contours represent radio emission at levels of 7.5 and 50 mJy beam<sup>-1</sup>. Point sources identified with *wavdetect* but which are too faint to see in the smoothed image are marked with “+” symbols. The position of the OH maser is marked with a “X” symbol. X-ray emission seen in the northeast and southeast corners of the image is due to the large exposure correction near the edges of the field of view, and does not correspond to real emission. Regions discussed in the text are indicated.